Lateral loading experiments for buried pipe in reinforced ground with geogrids under different hydraulic gradient

K. Ono
Kobe University, Japan (131a003a@stu.kobe-u.ac.jp)

Y. Yokota&Y. Itani
Kobe University, Japan (159a018a@stu.kobe-u.ac.jp, 112a051a@stu.kobe-u.ac.jp)

Y. Sawada&T.Kawabata
Kobe University, Japan (sawa@harbor.kobe-u.ac.jp, kawabata@kobe-u.ac.jp)

ABSTRACT: In internal pressure pipelines, thrust force acts on the pipe bends constantly, and displacement of the buried pipe is supported by passive earth pressure. It has been reported that the pipe bends largely displaced and separation of pipe joints occurred since lateral resistance force was reduced in liquefied ground. In Japan, the improvement of seismic resistance is strongly required because it is expected that the severe earthquake occurs in the near future. As a countermeasure against liquefaction, Japanese current design standard for irrigation pipelines suggests the method that pipelines are partially backfilled with gravel to enhance the capability of dissipation of pore water pressure. In addition, the past researches show that thrust restraints using geogrids and gravel in liquefied ground are very effective since pull-resistive stress of the geogrids prevents the displacement of bent pipe. However, the details of the design methods about the appropriate installation area of gravel and geogrids are still not clear, and the specific guideline for practical usage is not established. In the present study, the lateral loading tests are carried out in order to correct the knowledge which contributes to developing the liquefaction countermeasures using geogrids and gravel. The test results show that the countermeasure method which integrated the gravel surrounding the pipe was the most effective to enhance the shear resistance force against the displacement of the pipe.

Keywords: Pipeline, Liquefaction, Geogrid, Model experiment, Horizontal resistance force

1 INTRODUCTION

In internal pressure pipelines, thrust force constantly acts on the pipe bends, and the force is supported by the passive earth pressure of the ground. If the passive earth pressure is insufficient to support the thrust force, it is general to attach a concrete block at the pipe bend to increase the contact pressure. Although the effectiveness of thrust restraint using the concrete block was verified by many past researches, a decrease in the passive earth pressure due to liquefaction is not taken into consideration. In the Hokkaido-Nansei-Oki earthquake in Japan in 1993, large displacement of the concrete block at the pipe bend and the separation of the pipe joints were reported in the liquefied ground (Mohri et al, 1995). Pipelines suffered similar damages by the 2011 off the Pacific coast of Tohoku Earthquake, and it was revealed that the concrete block became the weak points during earthquakes for the pipelines because the response acceleration against the seismic waveform was different (Ariyoshi et al., 2012). In Japan, the improvement of the seismic resistance is strongly required because it is expected that the severe earthquake will occur in the near future.
Japanese current design standard for irrigation pipelines (2009) suggests the countermeasure methods that partially backfill pipelines with the gravel to enhance the capability of the dissipation of the excess pore water pressure. Ling et al. (2003) simulated the seismic performance of a large-diameter buried pipe using the shaking table on the centrifuge, and verified that the countermeasure method using gravel and geogrid was effective against the flotation of the pipe. Kawabata et al. (2009, 2011) proposed the thrust protecting method using geogrid which took the

place of the method with the concrete block. Experimental results revealed that the thrust protecting method with geogrid and gravel was very effective during earthquake since pull-resistive stress of geogrids prevented the displacement of the pipe bends in the liquefied ground. However, the details of the design methods about the appropriate installation area of the gravel and the geogrid are still not clear, and the specific guideline for the practical usage has not been established.
In the present study, the model experiments are carried out in order to correct the knowledge which contributes to developing the liquefaction countermeasures using geogrids and gravel.

2 OUTLINE OF EXPERIMENT

2.1 *Experimental setup*

The schematic diagram of the experimental setup is shown in Figure 1. The model setup was composed of the rigid aluminum box, the water tank, the model pipe, and the traction apparatus.
The rigid aluminum box had 600 mm in length, 200 mm in width, and 500 mm in height, and the front face of the box was made of acrylic in order to observe the behavior of the pipe and the ground during the experiment. To investigate the degree of liquefaction of the ground, fourteen pore pressure transducers were installed into the central section of the box in the depth direction. The water tank was connected to the bottom of the box with the tube.

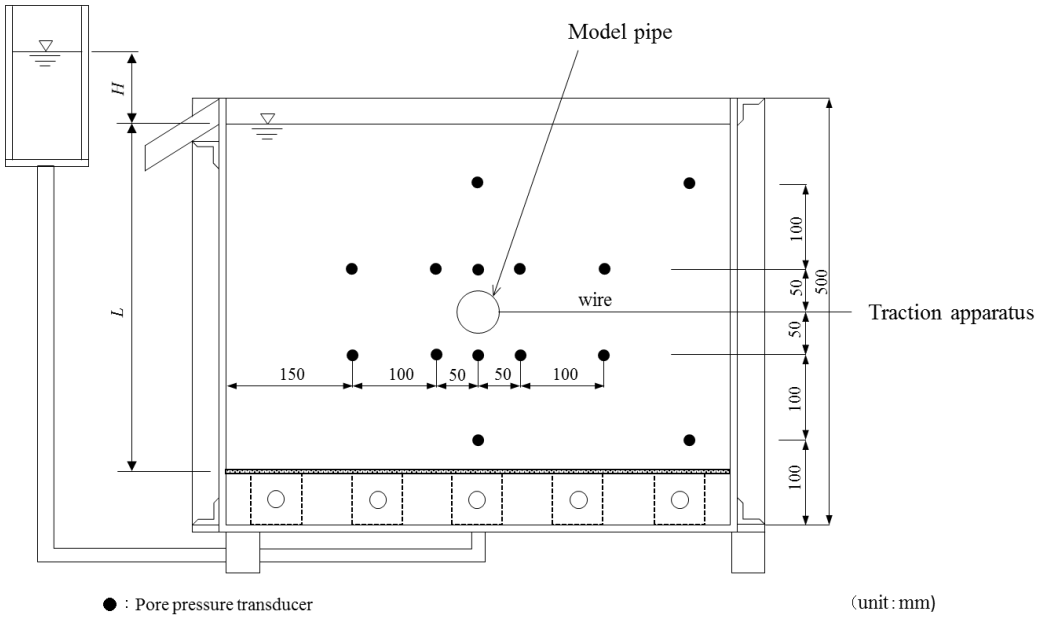

Figure 1: Experimental setup

The model pipe is shown in Figure 2. A pipe bend was modeled by the straight aluminum pipe having a diameter of 50 mm. The weight of the pipe was equal to the saturated unit weight of the sand. The nonwoven fabric sheets were attached on both ends of the pipe to reduce friction between the model pipe and the side walls of the box. The pore pressure transducers were installed at both sides of the pipe as shown in Figure 2.

Figure 2: Model pipe

Silica sand was used for the backfill. The model ground was prepared by a technique of water pluviation that produced a relative density of 40 %. As the backfill material around the model pipe, the silica sand and the gravel were used. The properties of the silica sand are presented in Table 1 and the grain size accumulation curves are shown in Figure 3. The geogrid used in the experiment was made of polyethylene and maximum tensile strength was 3.5 kN/m. The mesh size of the geogrid was 5 mm, and it was smaller than the diameter of the gravel.

Table 1. Properties of sand

Density of soil particle (g/cm^3)	2.64
Maximum dry density (g/cm^3)	1.58
Minimum dry density (g/cm^3)	1.23
Coefficient of uniformity	1.94

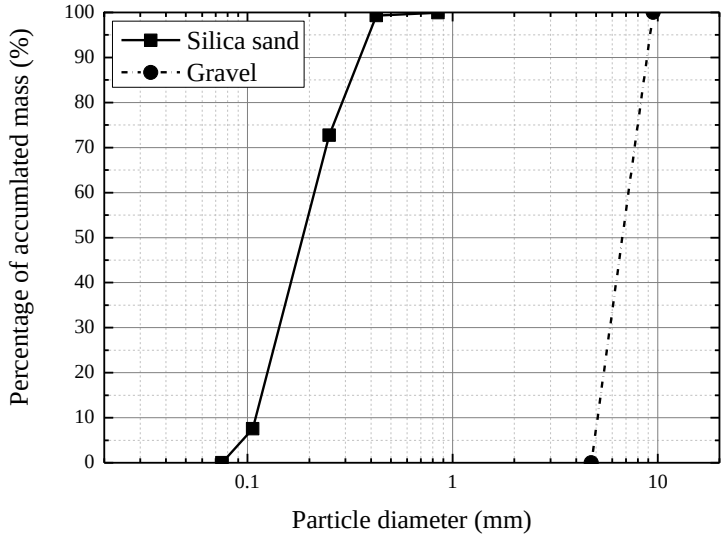

Figure 3: Grain size accumulation curve of sand and gravel

2.2 *Procedure of experiments*

In the present study, the ground was liquefied by raising the water level of the water tank and allowing the upward seepage to generate the excess pore water pressure in the ground. This method enabled the state of the ground to keep constant in comparison with using a shaking table.
After the hydraulic gradient ($i=H/L$) was kept constant, the pipe was pulled horizontally. The horizontal displacement of the pipe and the horizontal resistance force were measured. The loading rate of the pipe was kept constant at 0.1 mm/s in reference to similar lateral loading tests by Itani et al. (2015).
The backfill conditions are schematically illustrated in Figure 4. In Type-A, the pipe was buried without the countermeasure method. In Type-B, the layer of 50 mm around the pipe was backfilled with the gravel. In Type-C and Type-D, the layer of 50 mm around the pipe was integrated with the geogrid. In Type-E and Type-F, the pipe was integrated with the gravel in the upper part and the left side of the pipe. In all cases, the hydraulic gradient of the ground was set to i=0.0 and i=1.0.

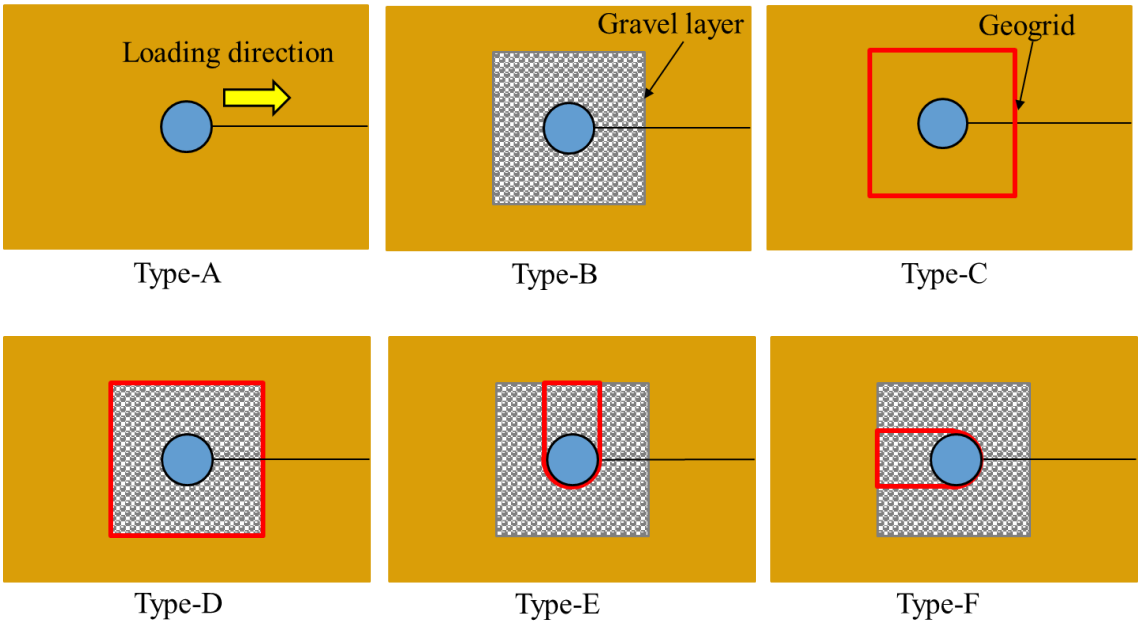

Figure 4: Backfill conditions

3 EXPERIMENTAL RESULTS

3.1 *Relationships between hydraulic gradient and excess pore water pressure ratio*

Figure 5 shows the relationships between the hydraulic gradient i and the excess pore water pressure ratio at the height of the center of the pipe. The excess pore water pressure ratio was defined as the excess pore water pressure normalized by the initial vertical effective stress. The excess pore water pressure was the increment from the pore water pressure of the saturated ground (i=0.0), and it was the mean value of the pore water pressure which was measured at the position of 200 mm and 300 mm in height. When the gravel was used as the backfill material around the pipe, only the value which was measured by the pore pressure transducers in the sand were used. Ideally, the excess pore water pressure ratio reaches 1.0 at the critical hydraulic gradient (i_{cr}=0.85), and this was illustrated as a critical line in the graph. The critical hydraulic gradient can be obtained from the following equation.

$$i_{cr} = \frac{G_s - 1}{1 + e} \quad (1)$$

Where G_s = specific gravity of sand and e = void ratio

In Type-A, the excess pore water pressure ratio increases along the critical line with the rise of the hydraulic gradient. The increment rate of the excess pore water pressure ratio decreases as the hydraulic gradient grows large, and the excess pore water pressure ratio does not reach 1.0 even if the hydraulic gradient raised up to 1.0. The ground was not liquefied completely because water path generated in the wall surface of the box.

In Type-B, the increment rate of the excess pore water pressure ratio is smaller than that in Type-A, and the difference is remarkable when the hydraulic gradient is more than 0.6. The excess pore water pressure ratio is about 0.75 when the hydraulic gradient is 1.0, and this value was almost equal to the excess pore water pressure ratio at i=0.7 in Type-A. It was because that the coefficient of permeability of the gravel was larger than that of the sand, and a lot of upward seepage flowed through the gravel layer. It was found that the increment of the excess pore water pressure ratio was reduced by using the gravel as a backfill material around the pipe.

The relationship between the hydraulic gradient and the excess pore water pressure ratio in Type-C was almost the same with the relationship in Type-A. It was found that the presence of the geogrid did not influence the relationship. In the case using the gravel as the backfill material, this tendency was similar.

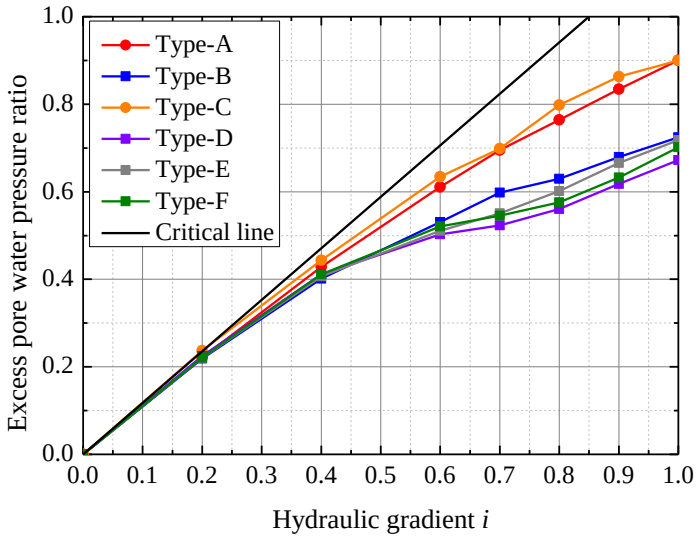

Figure 5: Relationships between hydraulic gradient and excess pore water pressure ratio

3.2 *Horizontal resistance force*

Figure 6 shows the relationships between the horizontal displacement of the pipe and the resistance force of the ground when the hydraulic gradient was 0.0. The horizontal resistance force was evaluated as the force per unit area.

The horizontal resistance force in Type-A is the smallest in all cases, and it was found that the countermeasure methods in Type-B, C, D, E, F gave the additional resistance force in the saturated ground. In Type-A and Type-B, the relationships between the displacement and the resistance force are non-linear, and the increment rate of the resistance force decreases as the displacement of the pipe increases. On the other hand, in Type-C and Type-D, the relationships are almost linear. Above results showed that the extension of the geogrid and the tensile force were in a linear relation.

The horizontal resistance force in Type-C is larger than that in Type-A. The difference increases with the increment of the displacement of the pipe because the geogrid extended depending on the pipe displacement. Judging from the results in Type-A, B, and C, the reinforcement effect by the geogrid was larger than the shear strength of the gravel in the saturated ground. On the other hand, the resistance force in Type-D is the largest in all cases. From the comparison between Type-C and Type-D, it was found that the backfill materials in the geogrid affected the resistance force. The sand particle in Type-C was easier to go through the mesh of the grid than the gravel in Type-D.

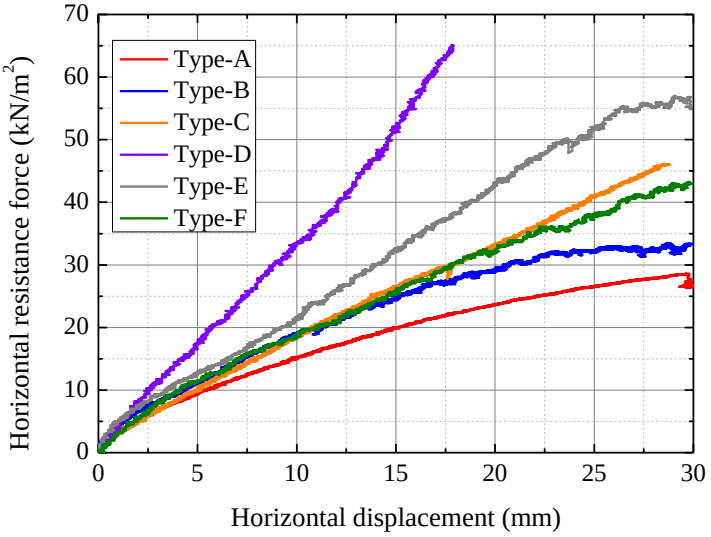

Figure 6: Horizontal resistance force (i=0.0)

The horizontal resistance force in Type-E and Type-F becomes larger than that in Type-B with the increase of the displacement of the pipe. As is the same with Type-C, the geogrid extended in response to the pipe displacement, and the tensile force was added.
The horizontal resistance force in Type-E is larger than that in Type-F. Since the volume of the integrated part in the geogrid was the same in Type-E and Type-F, this result suggested that the position of the geogrid and the horizontal projected area of the integrated part were more dominant than the total length of the geogrid.

3.3 *Coefficient of horizontal subgrade reaction*

Figure 7 shows the relationships between the excess pore water pressure ratio and the coefficient of horizontal subgrade reaction. The subgrade reaction was calculated as below.

$$k = \frac{F}{\delta \cdot A} \tag{2}$$

Where F = resistance force, δ = horizontal displacement of pipe, and A = projected area of pipe

In the present paper, we chose the resistance force at 15 mm for the calculation because the difference among the countermeasure methods was apparent judging from Figure 6. The all experimental results were plotted with the approximate lines estimated by a least-squares method.
In every case, the subgrade reaction linearly decreases as the excess pore water pressure ratio increases. The effective stress of the ground decreased due to the rise of the excess pore water pressure, and thereby the shear resistance force of the ground largely declined.
In addition, although the difference of the subgrade reaction due to the countermeasure methods is confirmed in the saturated ground (excess pore water pressure is 0.0), there is no significant difference in the completely liquefied ground (excess pore water pressure is 1.0) except Type-D. It was expected that the shear resistance force of the gravel did not develop sufficiently during liquefaction because the surrounding sandy ground liquefied and largely lost the shear resistance force. However, as shown in the relationships between the hydraulic gradient and the excess pore water pressure in Figure 5, it is hard to expect that the ground with gravel will completely liquefy because the gravel zone has dissipating effect of the excess pore water pressure. In other words, as the effectiveness of the gravel, the requirement to take into account the resistance force of the gravel during complete liquefaction is relatively low.
In Type-D, the decline rate of the subgrade reaction against the excess pore water pressure ratio is smaller compared to the other cases. Since the surrounding area of the pipe was integrated with the gravel and the geogrid, the passive ground avoided large deformation and maintained the enough high shear resistance force. Judging from the above, the countermeasure method which integrated the gravel surrounding the pipe was the most effective to enhance the shear resistance force against the displacement of the pipe.

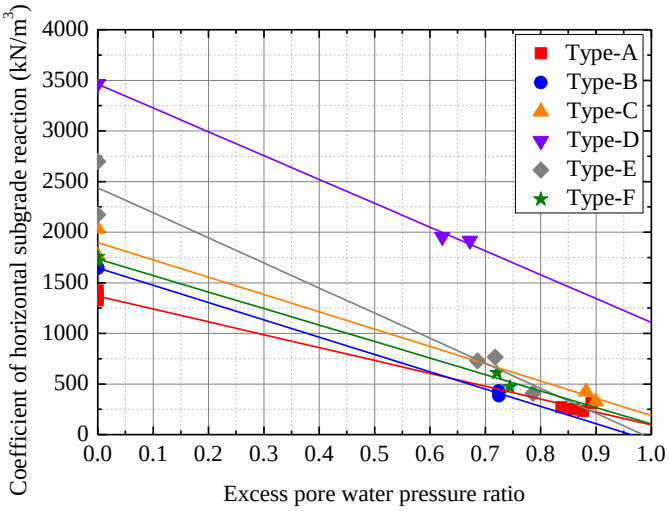

Figure 7: Coefficient of horizontal subgrade reaction

3.4 *Vertical displacement of pipe*

The relationships between the horizontal displacement and the vertical displacement of the pipe at i=0.0 and i=1.0 are shown in Figure 8 and Figure 9, respectively.

In Type-A, the pipe uplifts about 4 mm when the horizontal displacement is 30 mm at i=0.0, while the pipe uplifts only 0.5 mm at i=1.0. The maximum settlement of the pipe is about 1 mm when the hydraulic gradient is 0.0, while it is about 2.5 mm when the hydraulic gradient is 1.0. It was found that the settlement of the pipe increased with the increment of the liquefaction degree of the ground because the bearing capacity of the ground under the pipe significantly decreased due to liquefaction. In Type-B, the relationships between the degree of liquefaction of the ground and the vertical displacement are similar to that of Type-A. This result showed that the relationship was not dependent on the backfill materials. In comparison between Type-A and Type-B in the saturated ground, the settlement of the pipe in Type-A is slightly larger than that of Type-B, and the floating amount of the pipe in Type-A is smaller than that of Type-B. On the other hand, the vertical displacement in Type-A is almost equal to that in Type-B in the liquefied ground. From these results, the effectiveness of the gravel which prevented the pipe from moving horizontally faded off in the liquefied ground.

By contrast, in Type-C, D, E, F, although the settlement of the pipe decreases by reinforcing with the geogrid, the floating amount of the pipe increases. The floating of the pipe was promoted since the resistance force acting on the pipe increased. In particular, the floating amounts of the pipe in Type-D and Type-F are large. It indicated that the horizontal length of the geogrid significantly affected the vertical displacement of the pipe. We need to develop a new method which prevents the pipe from floating.

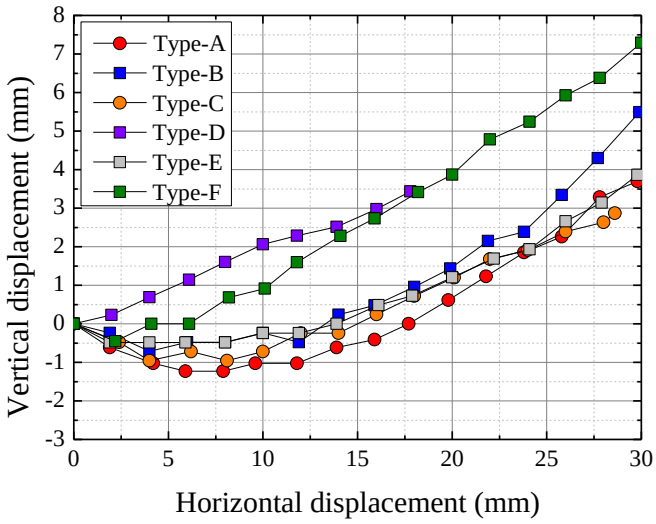

Figure 8: Relationships between the horizontal displacement and the vertical displacement of the pipe (i=0.0)

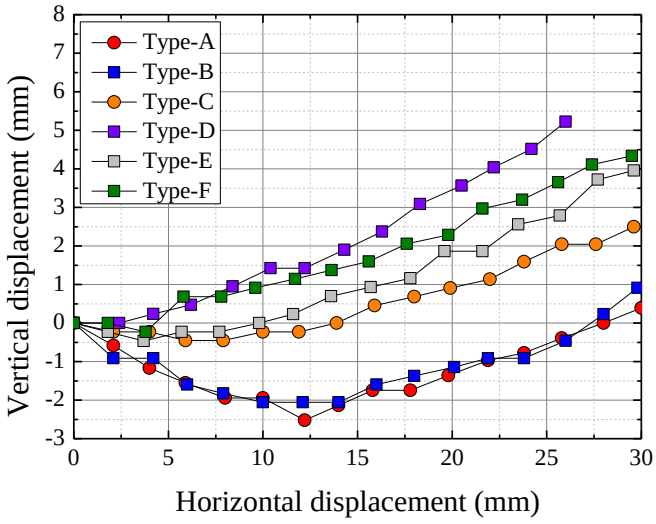

Figure 9: Relationships between the horizontal displacement and the vertical displacement of the pipe (i=1.0)

3.5 *Deformation of gravel and geogrid*

Figure 10 shows the pictures of the pipe in the liquefied ground (i=1.0) when the displacement of the pipe was 0 mm and 25 mm in Type-B, C, D, E, F. The blue line and the white line on the pictures show the deformation shape of the gravel and the geogrid, respectively.

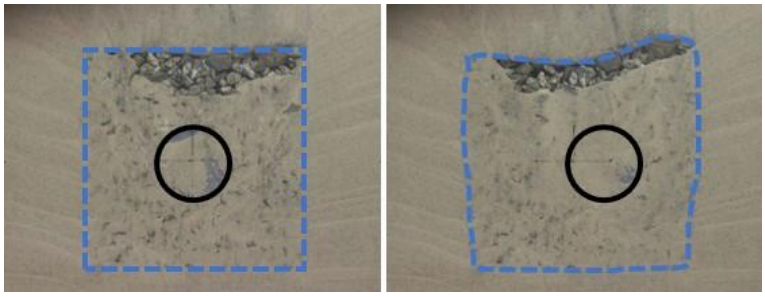

(a) Type-B

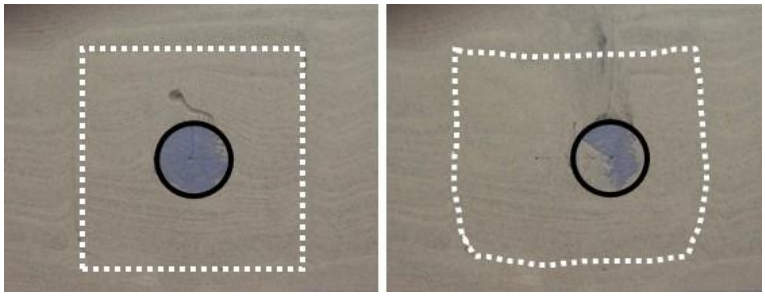

(b) Type-C

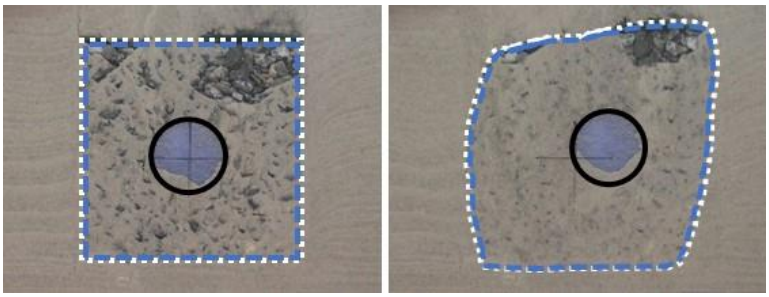

(c) Type-D

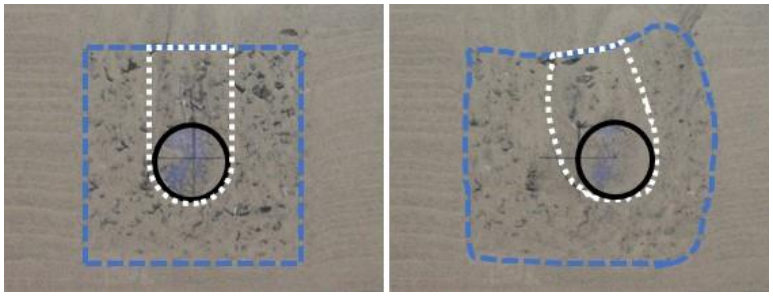

(d) Type-E

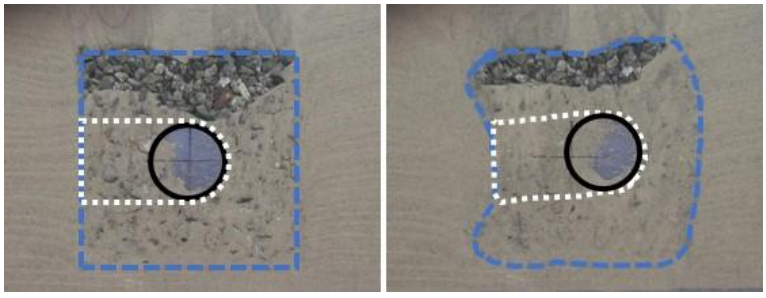

(e) Type-F

(left:0 mm, right:25 mm)

Figure 10: Pictures of pipe in liquefied ground

In Type-B, the gravel in the right side of the pipe is pushed upward by the pipe displacement, and the gravel above the initial position of the pipe sinks. The gravel in the left side and the bed of the pipe hardly transforms.
In Type-C, the geogrid extends horizontally, and the right end of the geogrid changes into a bow shape. Although the distance between the pipe and the right-end geogrid narrows, the geogrid is not extended vertically. This result showed that the sand particle passed through the mesh of the geogrid, and the sand was not restrained sufficiently by the geogrid. On the other hand, in Type-D, the gravel and the geogrid in the upper right corner are pushed upward by the pipe, and the geogrid in the upper left corner is pulled to the right. The gravel just above the initial position of the pipe does not sink, and this means that the gravel around the pipe displaced with the displacement of the pipe by the integrated effect of the geogrid.
In Type-E, the top end of the geogrid hardly displaces and the left side of the geogrid is significantly extended with the displacement of the pipe. The extension of the geogrid contributed to the increment of the horizontal resistance force. On the other hand, in Type-F, the left end of the geogrid does not displace vertically, but it displaces horizontally with the pipe. The deformation of the geogrid was not large in comparison with that in Type-E, and it indicated that the tensile resistance force by the extension of the geogrid was smaller than that in Type-E.

4 CONCLUSIONS

In the present study, the lateral loading tests were carried out in order to correct the knowledge which contributes to developing the liquefaction countermeasures using the geogrid and the gravel. The following conclusions were obtained from the study:

1. The increment of the excess pore water pressure ratio reduced by using the gravel as a backfill material around the pipe. The presence of the geogrid did not influence the relationship between the hydraulic gradient and the excess pore water pressure ratio.
2. In the saturated ground, the horizontal resistance force increased by using the gravel and the geogrid, and the reinforcement effect by the geogrid was larger than the shear strength of the gravel. In the case with geogrid, the backfill materials in the geogrid affected the resistance force.
3. In the liquefied ground, the countermeasure method which integrated the gravel surrounding the pipe with the geogrid was the most effective to enhance the shear resistance force against the displacement of the pipe. In the liquefied ground, the coefficient of subgrade reaction of other countermeasure methods was almost equal to that in the case without the countermeasure.
4. In the case without the countermeasure methods, the settlement of the pipe increased with the increment of the liquefaction degree of the ground. In the case with the gravel as the backfill material, this tendency was similar. Although the settlement of the pipe decreased by reinforcing with the geogrid, the floating amount of the pipe increased.

REFERENCES

Ariyoshi, M., Mohri, Y., Asano, I. and Ueno, K. (2012) Damage and Restoration of Agriculture Pipeline at Kumadogawa Irrigation Project by the 2011off the Pacific coast of Tohoku Earthquake, *Technical report in NIRE*, .**213**, 201-215.(in Japanese)

Itani, Y., Fujita, N., Sawada, Y., Ariyoshi, M., Mohri, Y. and Kawabata, T. (2015) Model experiment on the Horizontal Resistance Force of Buried Pipe in Liquefied Ground, *IDRE Journal*, **295**, 77-83.(in Japanese)

Kawabata, T., Sawada, Y. and Mohri, Y. (2009) Large Scale Experiments on Lightweight Thrust Restraint for Buried Bend under Internal Pressure, *Transactions of The Japanese Society of Irrigation, Drainage and Reclamation Engineering*, JSIDRE, **262**, 111-117.(in Japanese)

Kawabata, T., Sawada, Y., Mohri, Y. and Ling, H. I. (2011) Dynamic Behavior of Buried Bend with Thrust Restraint in

Liquefying Ground, *Journal of Japan Society of Civil Engineers, Series C (Geosphere Engineering)*, **67**(3), 399-406.(in Japanese)

Ling, H. I., Mohri, Y., Kawabata, T., Liu, H., Burke, C. and Sun, L. (2003) Centrifuge Modeling of Seismic Behavior of Large-Diameter Pipe in Liquefiable Soil, *Journal of Geotechnical and Geoenvironmental Engineering*, ASCE, **129**(12), 1092-1101.

Ministry of Agriculture, Forestry and Fisheries of Japan (2009) Planning and Design Criteria of Land Improvement Project (Pipeline).(in Japanese)

Mohri, Y., Yasunaka, M. and Tani, S. (1995) Damage to Buried Pipeline Due to Liquefaction Induced Performance at the Ground by the Hokkaido-Nansei-Oki Earthquake in 1993, *Proceedings of First International Conference on Earthquake Geotechnical Engineering*, IS-Tokyo, 31-36.